Is there a direct solar proton impact on lower stratospheric ozone?

Jia Jia[1], Antti Kero[1], Niilo Kalakoski[2], Monika E. Szeląg[2*], Pekka T. Verronen[1,2]

[1] Sodankylä Geophysical Observatory, University of Oulu, Sodankylä, Finland
[2] Space and Earth Observation Centre, Finnish Meteorological Institute, Helsinki, Finland
[*]earlier known as M. E. Andersson

Correspondence to: Jia Jia (jia.jia@oulu.fi)

Abstract. We investigate Arctic polar atmospheric ozone responses to Solar Proton Events (SPEs) using MLS satellite measurements (2004-now) and WACCM-D simulations (1989-2012). Special focus is on lower stratospheric ozone depletion that has been proposed earlier based on superposed epoch analysis of ozonesonde anomalies (up to 10% ozone decrease). Superposed Epoch Analysis (SEA) of the satellite dataset provides no evidence of any average SPE impact on the lower stratospheric ozone, although at the mesospheric altitudes a statistically significant ozone depletion is present. In the individual case studies, we find only one potential case (January 2005) in which the lower stratospheric ozone level was significantly decreased after the SPE onset. However, similar decreases could not be identified in other SPEs of similar or larger magnitude. We find a very good overall consistency between SPE-driven ozone anomalies derived from the WACCM-D model simulations and the Aura MLS data. The simulation results before the Aura MLS era indicate no significant effect on the lower stratospheric ozone either. As a conclusion, the SPE has a zero direct impact on the lower stratospheric ozone.

1 Introduction

In the near-Earth space, solar wind charged particles are guided by the Earth's magnetic field and are able to precipitate into the middle and upper atmosphere in the polar regions. Such kind of precipitation creates the spectacular aurora, but also produces considerable amounts of HO_x (H, OH, HO_2) and NOx (N, NO, NO_2) through ion-neutral chemistry (e.g. Verronen and Lehmann, 2013). HO_x and NO_x increases lead to ozone loss through catalytic reactions in the mesosphere and upper stratosphere, respectively (Sinnhuber et al., 2012). Moreover, in polar winter, NO_x has a long chemical lifetime due to limited photodissociation by solar radiation. NO_x produced by energetic particle precipitation (EPP) in the mesosphere-lower thermosphere is transported down to the stratosphere by the Brewer-Dobson circulation inside the polar vortex (Funke et al., 2014), causing depletion of upper stratospheric ozone (Damiani et al., 2016). A number of studies have confirmed EPP's remarkable role in ozone depletion directly during large EPP events (e.g. Funke et al., 2011) and in-directly due to descending NO_x (e.g., Randall et al., 2007). Thus, most advanced climate models are now including EPP forcing, in order to correctly represent the ozone distribution in the polar stratosphere and mesosphere (Matthes et al., 2017; Stone et al., 2018).

Solar proton events (SPE) are one of the main types of EPP. During SPE, particles (mainly protons, ~10% alpha) with energies from tens to hundreds of MeV precipitate into the atmosphere at geomagnetic latitudes larger than 60° for days. Such high-energy particles mainly deposit their energy at altitudes of 35-90 km, providing direct ionization forcing on the polar middle atmosphere. Large SPEs have been studied since the 1960s until today using satellite observations and model simulation. In addition to tens of percent of ozone loss observed at many altitudes (Jackman 2001, Seppälä et al. 2004, Verronen et al. 2006), a strong SPE can reduce total ozone by 1-3% for months after the event (Jackman 2011, 2014).

Recently, Denton et al. (2018 a, b) presented statistical studies of average ozone changes from 191 SPEs between 1989-2016 using ozonesonde measurements. Superposed epoch analysis of ozone anomalies at polar stations (Sodankylä, Ny-Ålesund, and Lerwick) indicated that SPEs occurring during winter are causing ozone decrease by 5-10%, on average, at 20 km altitude. This effect is not produced in the current models because SPE-induced ionisation rates are insignificant at this altitude even during largest events (Jackman et al., 2011), and Denton et al. included also a large number of very small SPEs in their analysis. Such ozone decreases has not been observed in the case studies of very extreme SPEs, e.g., the 2003 'Halloween' event, from either simulation or satellite observation (Funke et al. 2011, and references therein). Recently, statistical analysis based on simulations has found no evidence of such low-altitude ozone impact (Kalakoski et al. 2020).

Here we investigate the proposed SPE-induced direct depletion on lower stratospheric ozone using ozone data from the Microwave Limb Sounder (MLS) instrument aboard the Aura satellite and the Whole Atmosphere Community Climate Model (WACCM-D) simulations. We proceed to evaluate ozone changes at altitudes 10-70 km caused by SPEs both statistically (superposed epoch analysis) and individually (case by case). The MLS ozone data, WACCM-D atmospheric simulation, and SPE data sets are presented in Sect. 2. In order to cross-check ozone depletion at 20 km reported based on the ozonesonde data, statistical ozone responses from MLS satellite measurements are firstly provided in Sect. 3. Following that, ozone changes after individual SPEs are given in Sect. 4. Finally we summarize our results and conclusions in Sect. 5.

2   Data sets

2.1   O$_3$ profile measurements by MLS

The Microwave Limb Sounder (MLS) onboard the Earth Observing System (EOS) Aura satellite measures ozone emission at 240 GHz, providing ozone volume mixing ratios at 55 pressure levels since 15 July 2004 (Waters et al., 2006). Vertical profiles are retrieved from the MLS observations with a 165 km horizontal spacing at altitudes between 8 and 90 km, a spatial resolution of 500 km × 500 km (along-track × across-track), and a vertical resolution of ~3.2 km. In this work, we use version 4.2 ozone data measured at 261 - 0.02 hPa (~10 - 70 km) to calculate the daily averaged ozone density profile at northern high latitudes (60°-90°N). Readers who are interested in the MLS data quality are referred to Livesey et al. (2018).

2.2   O$_3$ from WACCM-D simulations

WACCM is a global circulation model, including fully coupled dynamics and chemistry. Here, we use version 4 of the WACCM with resolution of 1.9° latitude by 2.5° longitude, with 88 vertical levels reaching from surface to 6×10^{-6} hPa (≈140 km). Overview of the model and the description of climate and variability in long-term simulation was presented by Marsh et al. (2013), with details of model physics in MLT (mesosphere - lower thermosphere region) and the response of the model to radiative and geomagnetic forcing during solar maximum and minimum described by Marsh et al. (2007). The simulation results presented here are from WACCM-D, a variant of WACCM with more detailed set of lower ionospheric chemical reactions, aimed at better reproduction of observed effects of EPP on MLT neutral composition (Verronen et al. 2016, Andersson et al. 2016).

We use SD-WACCM-D specified dynamics configuration, with Modern-Era Retrospective Analysis for Research and Applications (MERRA) (Rienecker et al., 2011) meteorological fields to force dynamics at every time step up to about 50 km. Simulation covers years 1989-2012, and uses forcings from auroral electrons (E<10keV), solar protons (< 300 MeV), and galactic cosmic rays for energetic particle precipitation. The SPE ionization rates are based on proton flux measurements from the Geostationary Operational Environmental Satellites (GOES) (see e.g. Jackman et al., 2011, for the calculation method). The WACCM-D SPE effects on neutral species are compared to satellite observations in Andersson et al. (2016). Note that WACCM-D has not been validated below 20 km. Nevertheless, in Andersson et al (2016) the HNO$_3$ response above 15 km to single SPE onset was reasonable comparing to MLS data. We also stress that protons >300 MeV are not included in the simulation, as the contribution of >300 MeV protons to direct ozone loss in the lower stratosphere would likely be negligible due to the relatively small fluxes at such high energies (Jackman et al., 2011). For more details of the simulation setup, see Kalakoski et al. (2020).

2.3   Solar proton events

The data of solar proton events (SPEs) used in this study is based on NOAA GOES (Geostationary Operational Environmental Satellite) proton flux observations. Fig. 1 presents 261 SPEs recorded from 1975 to date, including their onset time, fluxes detected in space, approximated time of duration, and ionization rates to the atmosphere. Here, the onset of a SPE is defined as the time when 5-min average proton fluxes with energies >10MeV are greater than 10 Particle Flux Units (1 pfu = 1 particle /cm^2/s/sr) at the geosynchronous orbit. For the estimation

1 of SPE duration and its impact on the atmosphere, we use the daily average ion pair production rates at ~1 hPa.

2 These ionization rates are calculated from GOES proton flux observations using the energy deposition methodol-

3 ogy described in, e.g., Jackman et al. (2011). Our study uses 49 events that occurred after the launch of Aura

4 MLS (July 2004 - now) and 177 events that occurred in WACCM-D simulation period (Jan 1989 - Dec 2012) to

5 evaluate the ozone changes following SPEs. It is clearly demonstrated in Fig. 1 that these SPEs are more frequent

6 near solar maximum years. Majority of the events are with flux less than 400 pfu, and their impacts to the atmos-

7 phere below 1 hPa (~50 km) are small. It is worth to mention that although these SPEs seem to have no preference

8 in occurring season, their seasonal distribution varies by months and should be considered during the interpreta-
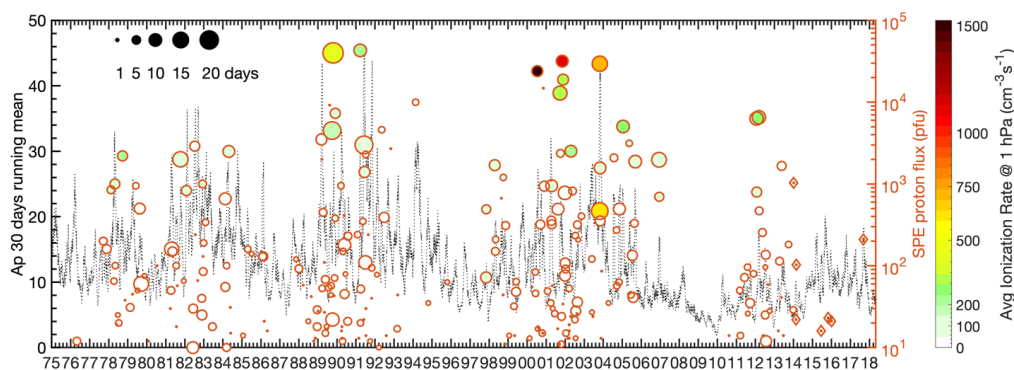
9 tion (Fig. A1).

Figure 1. Onset time of SPEs and their proton fluxes since 1975. The filled colors are the averaged ionization rate

during each SPE at 1hPa, while the size of the markers represents the approximate duration time of the SPEs obtained

from the 1hPa daily mean ionization rate. Diamonds mark the events without ionization information. The black dotted

line in the background is the 30-day mean of the daily geomagnetic activity Ap-index.

3 Statistical O$_3$ response from MLS

Similar to the method used by Denton et al. (2018 b), we applied a superposed epoch analysis to the MLS daily

ozone anomalies. The superposed epoch analysis, also referred to as compositing in geophysics, is used to acquire

variation of a time series before and after an event or a chain of certain kind of events. The point of time when the

event begins is the epoch time. In this case, the epoch times are the onset times of individual SPEs during MLS

operating period. All available ozone data were binned as a function of epoch time and altitude, with temporal

resolution of one day. The pre- and post-epoch spans used here are 30 and 60 days, respectively. For the selected

sets of SPEs, all the binned ozone data sets were averaged to represent the effect of the SPEs. This method ex-

cludes natural ozone variations that are larger than the span-scale. Since SPE-driven effects are expected to take

place on daily to monthly time scales, variations caused by e.g. QBO can be excluded. However, seasonal varia-

tions, must be excluded before using superposed epoch. Thus, the daily profile climatology calculated from the

ozone data was subtracted from the daily ozone data.
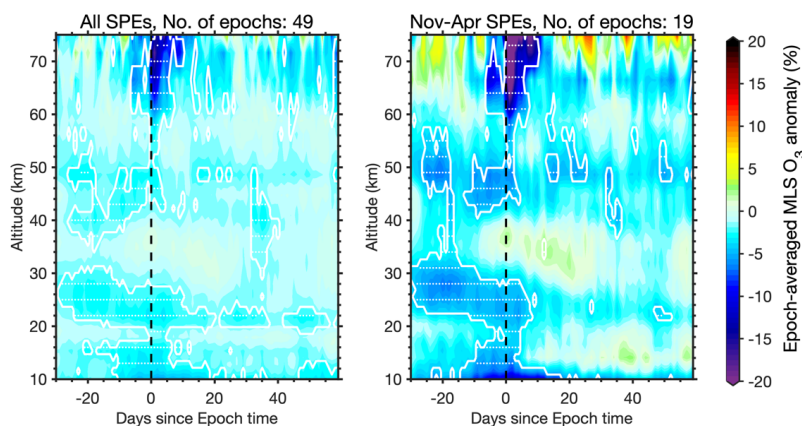
Figure 2. Epoch-averaged MLS ozone anomalies in the northern polar region (60°-90°N) (relative in %) along with geopotential altitude for a total of 49 SPE epochs (left panel) and 19 winter SPE epochs (right panel). The black dashed line represents the epoch time, i.e., onset of SPEs. The white thick line area corresponds to the epoch-averaged anomalies with >95% confidence after the Monte Carlo test.

In order to test the statistical significance of the obtained results, a Monte Carlo test was implemented. Instead of using SPE onset as epoch times, the analysis was rerun using 2000 random sets of epoch times. SPE-epoch averaged variations larger than 95% of the 2000 randomized results are considered significant and robust (reported as >95% confidence), suggesting that these extracted signatures are likely related to SPE.

Fig. 2 shows the superposed epoch of MLS northern polar ozone anomalies for all 49 SPEs (left panel) and for the ones occurred in winter (Nov-Apr) (right panel) within the instrument's operational period. Robust averaged anomalies (>95% confidence) are presented within the white thick lines. Spatial distribution of statistically robust anomalies is similar in all-SPE epochs and winter-SPE epochs. The depletion is more pronounced for winter epochs due to two facts: 1) ozone recovery is slower due to less production from O_2 photodissociation; 2) Largest SPEs with flux >1000 pfu that cause more ozone depletion happen to occur in NH winter. Among all the SPEs during MLS measurement period, ~3/4 of big SPEs are in NH wintertime (see Fig. A1). In both panels, closely following the SPE onset, very pronounced ozone depletion appears above 50 km for over 5 days. This is the direct ozone loss caused by the SPE-induced HO_x enhancement. The number of extreme SPEs is relatively small, which explains the absence of the long-lasting ozone depletion that would be expected between 40-50 km from enhanced amounts of NO_x. While the upper stratospheric ozone depletion signature is not seen in the statistical average, 5-10% decrease of ozone is present below 30 km, including ozone loss around 20 km similar to that reported by Denton et al. However, although the decrease of ozone at 20 km does appear after the epoch time, the signatures above and below are not related to the epoch times. This suggests that the whole robust variation in the stratosphere is more related to other phenomena in the northern polar cap, e.g. to changes in the strength of polar vortex or related chemical effects. We will discuss this in more detail in Sect. 4.

A superposed epoch analysis of WACCM-D ozone anomalies from SPEs during 1989-2012 has been reported by Kalakoski et al. (2020), thus we will not repeat it here. In their results, the epoch-averaged WACCM-D ozone

1   anomalies showed the same robust depletion at above 50 km. Since their analysis included also the very large

2   SPEs that occurred 1989-2004 (see Fig. 1 in this study and list of largest 15 SPEs in Tab. 1, Jackman et al., 2008),

3   long-term ozone depletion in the upper stratosphere was clearly detected as well. However, there was no robust

4   ozone loss below 30 km found in the WACCM-D simulations.

5   **4 O_3 response to individual SPEs**

6   Despite the fact that our WACCM-D epoch analysis includes most of the major SPEs in the space age, there is a

7   chance that ozone loss around 20 km may occur following individual large SPE in MLS data but the signal is

8   buried in all-event statistics, like in the case of upper stratospheric ozone depletion signatures. To exclude such a

9   possibility, in this section we analyse ozone responses to individual SPEs.
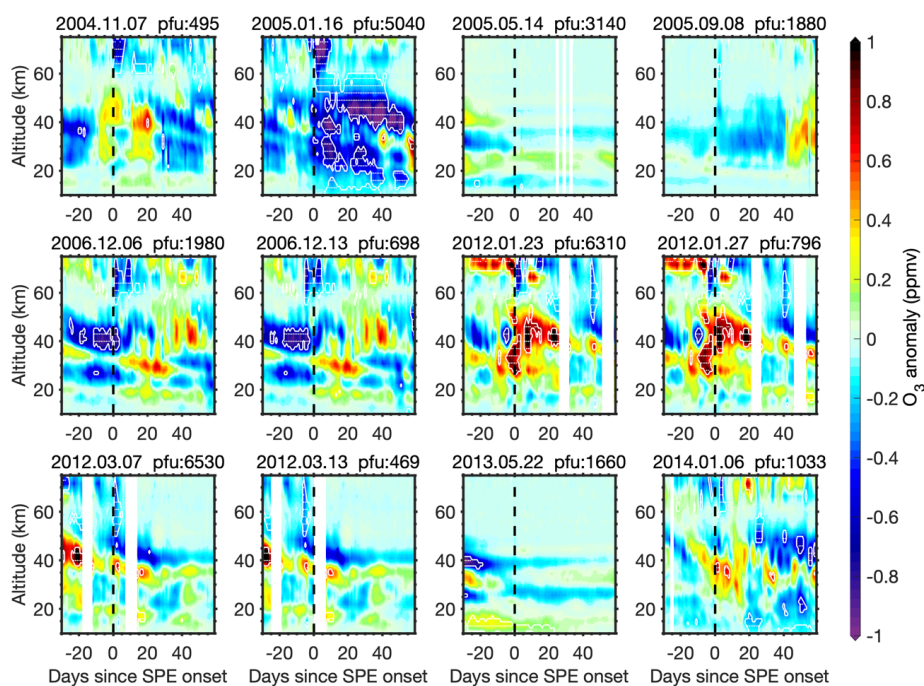
11   **Figure 3. MLS ozone anomalies (in ppmv) along with altitude at 30 days before and 60 days after individual big SPEs**

12   **(proton fluxes >400 pfu) since July 2004. The white thick line area demonstrates ozone anomalies with >95% confidence**

13   **after the Monte Carlo test.**

15   Similar to the analysis presented in Sect. 3, ozone anomalies presented here were calculated by subtracting daily

16   climatology from daily averaged ozone data from MLS and WACCM-D. Note that the subtracted daily mean

17   climatology from MLS and WACCM-D were derived from the MLS data period and the WACCM-D simulation

18   period, respectively. Then, instead of applying superposed epoch analysis on multiple SPEs, ozone anomalies are

19   presented 30 days before and 60 days after onset of individual SPE. For estimating the statistical significance of

1   the ozone anomalies found in the individual SPEs, we applied a similar Monte Carlo approach as in the case of

2   SEA, i.e., the variance of 6000 random 'onset' times was used as a measure for a significant anomaly. It is worth

3   noting, however, that this method recognizes 'statistically significant' all anomalies larger than the random back-

4   ground variation, whether the anomaly is due to SPE or, for instance, due to exceptional dynamical/chemical

5   anomalies, which have a similar occurrence probability as SPEs.

6   Anomalies following all individual SPEs can be found in Figs. A2 and A3. In general, SPEs with proton fluxes <

7   400 pfu cause neither visible daily ozone depletion in the mesosphere (below 75 km), nor in other altitudes. Ozone

8   changes following individual SPEs are more pronounced during winter. Figs. 3 and 4 demonstrate MLS and

9   WACCM-D ozone variations following SPEs with proton fluxes > 400 pfu since July 2004. Both the ozone vari-

10   ations and the robust signatures from these two different data sets are very consistent. After year 2004, three large

11   winter SPEs, i.e., January 2005, September 2005 and March 2012, produced clear upper stratospheric ozone loss.

12   Ozone depletion is most pronounced following the January 2005 event. For this event, we also observe a robust

13   lower stratospheric ozone loss from MLS following SPE for the first time: ozone is depleted by ~1 ppmv (~15%)

14   at 20 – 35 km and by ~0.15 ppmv (> 20%) below 15km 5 days after SPE onset.
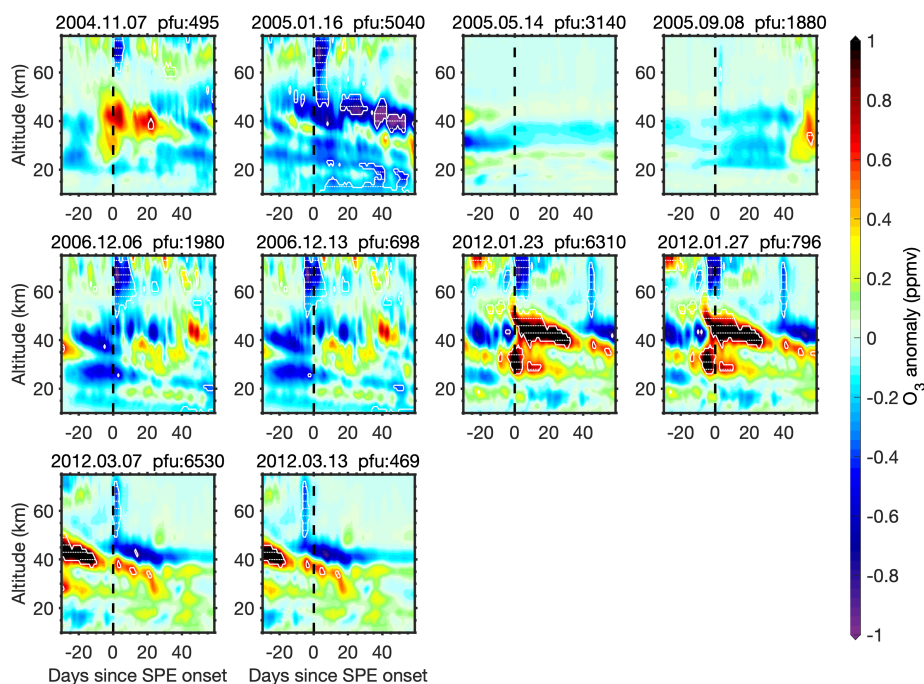
15

16   **Figure 4. Same as Fig. 3 but for WACCM-D ozone anomalies.**

17

18   Overall, wintertime ozone variation below 35 km is rather complicated. Year-to-year variability of stratospheric

19   polar ozone is mostly controlled by dynamical and chemical processes, both are essentially coupled to temperature

20   changes. Factors that modify polar temperature, e.g., sudden stratospheric warming (SSW) and El Niño–Southern

1   Oscillation (ENSO), are essentially planetary wave perturbations that modulate the strength of polar vortex. The

2   probabilities of major SSWs and, on the other hand, springs with extremely strong polar vortex are at similar

3   levels as the one of SPEs. Thus, ozone variations by these events will be seen as robust signatures in our study as

4   well, yet they do not necessarily coincide with onsets of SPEs with proton fluxes >400 pfu and >10000 pfu,

5   respectively. The large SPE in January 2012 (Figs. 3 and 4) is severe enough to destroy stratospheric ozone.

6   However, the stratospheric ozone anomalies at that time were dominated by dynamical ozone enhancement from

7   SSW in 17th Jan 2012 (Päivärinta et al., 2016). One of the most pronounced examples of extreme strong polar

8   vortex impact is the well-reported ozone depletion during spring of 2011, which can be observed in ozone anom-

9   alies around the two small SPEs that occurred in March 2011 (see Fig. A2). The lower stratospheric polar vortex

10 was the strongest (in either hemisphere) in the previous 32 years (Manney et al., 2011). Large volume of polar

11 stratospheric clouds (PSCs) converted chlorine reservoirs to ozone-destroying species, leading to extraordinary

12 low ozone in the stratosphere (Pommereau et al., 2018). Similarly, robust anomaly seen after January 2016 SPE

13 can be explained by cold 2015-2016 winter anomaly. We are confident to exclude SPE's influence on the anomaly

14 in both cases because: firstly, the signal is not following SPE onset, secondly these SPEs are such small events

15 that ozone loss was not observed, not even in the mesosphere. These robust non-SPE signals are included in the

16 superposed-epoch analysis performed in Sect. 3, contributing to the robust anomalies below 30 km in Fig. 2.

17
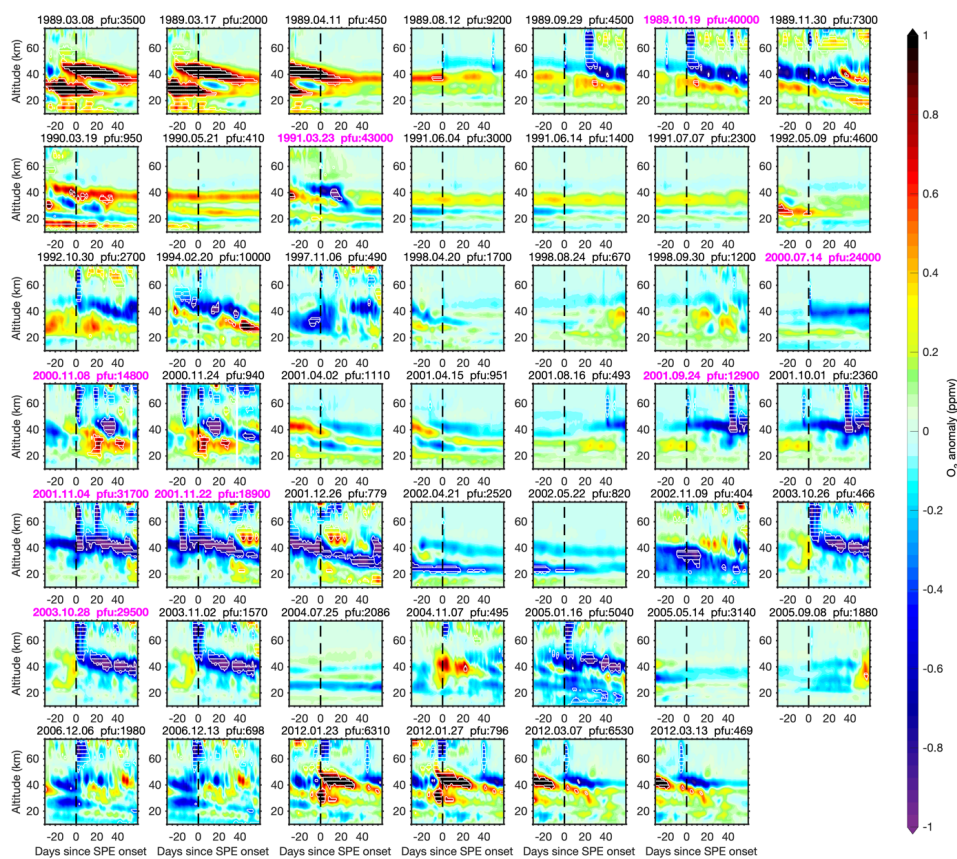
Figure 5. Same as Fig. 4 but for WACCM-D ozone anomalies before and after individual big SPEs (proton fluxes >400 pfu) since 1989. Extreme SPEs (proton fluxes >10000 pfu) are marked with bold magenta titles.

Identify sources of the robust ozone anomaly below 35 km following the SPE beginning on 16th Jan 2005 is difficult. With a moderate cold winter temperature causing more ozone loss, coincident of robust dynamical ozone changes following the SPE exists. Meanwhile, an extremely large (over 270%) ground level enhancement (GLE) of neutrons occurred during the SPE period on 20 January 2005 (Jackman et al., 2011). Ionization rate reached 500 cm-3s-1 at 30 km for one day due to the very high energy protons (300-20 000 MeV) that caused the GLE (Usoskin et al., 2011). Jackman et al. (2011) carried out a detailed study of January 2005 SPE's influence on the northern polar atmosphere using WACCM3 simulation, and reported an ozone column decrease of less than 0.01% by GLE protons, while the ozone changes below 50 km observed in MLS data are seasonal changes. Nonetheless, in our study the robust MLS ozone destruction signature in the lower stratosphere following the January 2005 SPE is extremely unique, not only when compared to other SPEs cases after 2004, but also when large and extreme SPEs before 2004 are included (see the WACCM-D simulation result presented in Fig. 5). Further research needs to be done to confirm the dynamical/chemical factors that led to ozone destruction below 35 km in January 2005.

5   Conclusions

Recent studies have reported up to 10% average decrease of lower stratospheric ozone at 20 km altitude following solar proton events (SPE). However, mechanisms which could cause such a large low-altitude impact are not clear. We used the Aura MLS satellite ozone datasets from 2004 to date and WACCM-D model simulations from 1989 - 2012 to analyse SPE-driven ozone changes. In our approach, stratospheric and mesospheric daily ozone anomalies (10-70 km) were examined over the epochs of SPEs by applying 1) a Superposed Epoch Analysis (SEA) for all the cases and 2) a case-by-case analysis for individual events. Statistical significance of the anomalies found in the ozone levels was estimated by employing a Monte Carlo approach.

Arctic polar ozone destruction in the mesosphere and upper stratosphere can be directly observed from satellite measurement anomaly, when following SPEs in September-April with proton fluxes >400 pfu and >1000 pfu, respectively. We observe 5-10% ozone destruction below 30 km altitude in MLS SEA results. However, the depletion appears before the epoch time, i.e. SPE onset. We argue that such lower stratospheric ozone losses are rather caused by unusually stable and strong polar vortex, together with sufficient ozone depleting reservoirs of chlorine. In the case by case study, we find a very good overall consistency between SPE-driven ozone anomalies derived from the WACCM-D model simulations and the Aura MLS data. This enables us to generalise the study also to the SPEs before the Aura MLS era. From 1989 to date, robust lower stratospheric ozone decrease after SPEs was observed only once in MLS ozone anomaly, i.e. following the January 2005 SPE. Ozone was depleted by ~1 ppmv (~15%) at $20 - 35$ km and by ~0.15 ppmv (> 20%) below 15km 5 days after SPE onset. Nevertheless, the exact mechanisms of the suggested lower stratosphere impact are currently unclear. The simulation results indicate that even for the strongest SPEs in our record, there is no significant effect on the lower stratospheric ozone as such. Although it remains unclear to what degree the lower ozone decrease in January 2005 was caused by the SPE, and how much due to natural variability, we suspect that the observed, statistically significant lower stratospheric ozone impact is most likely by chance coincident with the SPE epoch. Based on our analysis, we argue that SPE do not cause direct lower stratospheric ozone anomalies.

1   **Appendix**
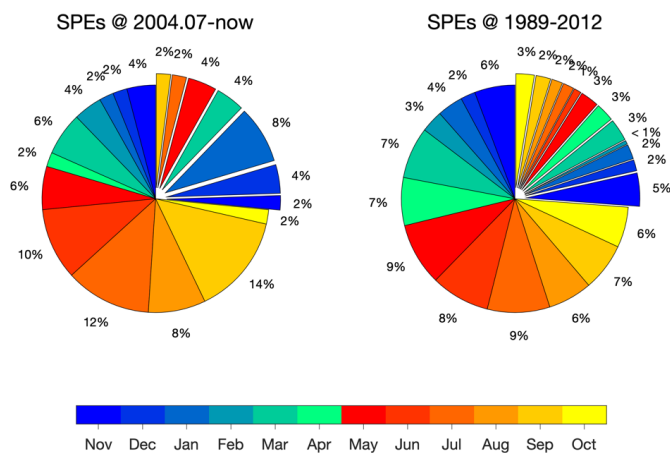
3   **Figure A1. SPE's seasonal distribution for those with fluxes >400 pfu (exploded parts of the pie chart) and the ones**

4   **with fluxes <400 pfu (regular parts of the pie chart). Left panel demonstrates the cases in between MLS measurement**

5   **period (2004.07- now). Right panel shows the cases during WACCM-D simulation (1989-2012).**
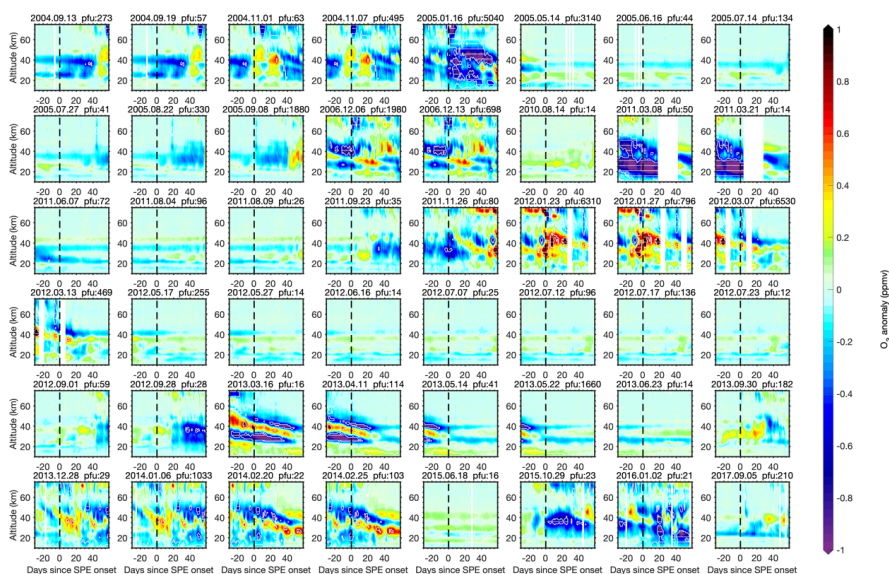
7   **Figure A2. Same as Fig. 3 but after all individual SPEs since July 2004.**
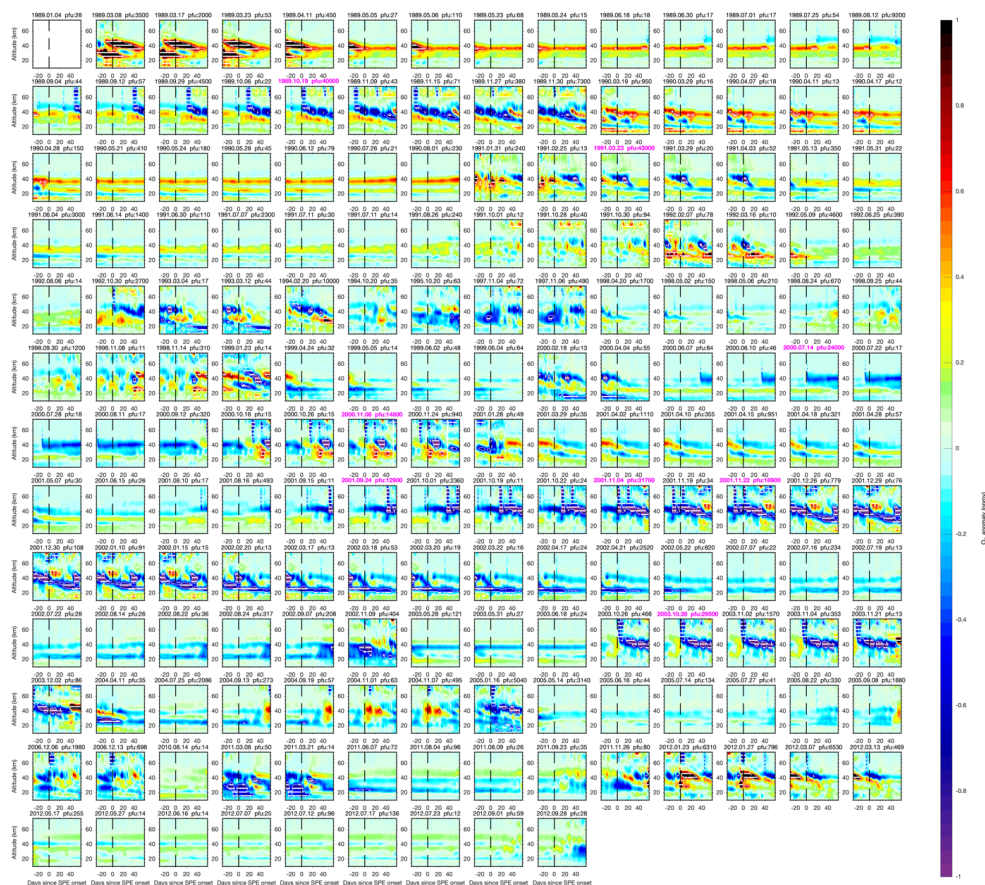
Figure A3. Same as Fig. 4 but after all individual SPEs since 1989.

Data availability

MLS ozone data used in this study is available at https://mls.jpl.nasa.gov/products/o3_product.php. Proton fluxes and solar proton events are available from https://www.ngdc.noaa.gov/stp/satellite/goes/index.html. Daily geomagnetic activity Ap-index used in Fig. 1 can be found at https://www.ngdc.noaa.gov/stp/GEOMAG/kp_ap.html. SPE induced ionization rate dataset is available at https://solarisheppa.geomar.de/solarprotonfluxes.

Acknowledgements

J. J. is funded by the University of Oulu's Kvantum Institute. The work of A.K is funded by the Tenure Track Project in Radio Science at Sodankylä Geophysical Observatory/University of Oulu. We would like to thank the MLS ozone teams for providing the ozone data. This work was carried out as a part of International Space Science Institute (ISSI) project "Space Weather Induced Direct Ionisation Effects On The Ozone Layer".

1 **References**

2 Andersson, M. E., Verronen, P. T., Marsh, D. R., Päivärinta, S., and Plane, J. M. C.: WACCM-D-Improved mod-

3 eling of nitric acid and active chlorine during energetic particle precipitation, J. Geophys. Res.-Atmos., 121,

4 10328–10341, https://doi.org/10.1002/2015JD024173, 2016.

5 Damiani, A., Funke, B., López Puertas, M., Santee, M. L., Cordero, R. R., and Watanabe, S.: Energetic particle

6 precipitation: A major driver of the ozone budget in the Antarctic upper stratosphere, Geophys. Res. Lett., 43,

7 3554–3562, https://doi.org/10.1002/2016GL068279, 2016.

8 Denton, M. H., Kivi, R., Ulich, T., Rodger, C. J., Clilverd, M. A., Horne, R. B., and Kavanagh, A. J.: Solar proton

9 events and stratospheric ozone depletion over northern Finland, Journal of Atmospheric and Solar-Terrestrial

10 Physics 177, 218-227, http://dx.doi.org/10.1016/j.jastp.2017.07.003, 2018 a.

11 Denton, M. H., Kivi, R., Ulich, T., Clilverd, M. A., Rodger, C. J., and von der Gathen, P.: Northern hemisphere

12 stratospheric ozone depletion caused by solar proton events: the role of the polar vortex, Geophys. Res. Lett., 45,

13 2115–2124, https://doi.org/10.1002/2017GL075966, 2018 b.

14 Funke, B., Baumgaertner, A., Calisto, M., Egorova, T., Jackman, C. H., Kieser, J., Krivolutsky, A., López-Puertas,

15 M., Marsh, D. R., Reddmann, T., Rozanov, E., Salmi, S.-M., Sinnhuber, M., Stiller, G. P., Verronen, P. T., Ver-

16 sick, S., von Clarmann, T., Vyushkova, T. Y., Wieters, N., and Wissing, J. M.: Composition changes after the

17 "Halloween" solar proton event: the High Energy Particle Precipitation in the Atmosphere (HEPPA) model versus

18 MIPAS data intercomparison study, Atmos. Chem. Phys., 11, 9089–9139, https://doi.org/10.5194/acp-11-9089-

19 2011, 2011.

20 Funke, B., López-Puertas, M., Stiller, G. P., and von Clarmann, T.: Mesospheric and stratospheric NOy produced

21 by energetic particle precipitation during 2002–2012, J. Geophys. Res.-Atmos., 119, 4429–4446,

22 https://doi.org/10.1002/2013JD021404, 2014.

23 Jackman, C. H., McPeters, R. D., Labow, G. J., Flem- ing, E. L., Praderas, C. J., and Russell, J. M.: Northern

24 hemisphere atmospheric effects due to the July 2000 Solar Proton Event, Geophys. Res. Lett., 28, 2883–2886,

25 https://doi.org/10.1029/2001gl013221, 2001.

26 Jackman, C. H., Marsh, D. R., Vitt, F. M., Garcia, R. R., Fleming, E. L., Labow, G. J., Randall, C. E., López-

27 Puertas, M., Funke, B., von Clarmann, T., and Stiller, G. P.: Short- and medium-term atmospheric constituent

28 effects of very large solar proton events, Atmos. Chem. Phys., 8, 765–785, https://doi.org/10.5194/acp-8-765-

29 2008, 2008.

30 Jackman, C. H., Marsh, D. R., Vitt, F. M., Roble, R. G., Randall, C. E., Bernath, P. F., Funke, B., López-Puertas,

31 M., Versick, S., Stiller, G. P., Tylka, A. J., and Fleming, E. L.: Northern Hemisphere atmospheric influence of the

32 solar proton events and ground level enhancement in January 2005, Atmos. Chem. Phys., 11, 6153–6166,

33 https://doi.org/10.5194/acp-11-6153-2011, 2011.

34 Jackman, C. H., Randall, C. E., Harvey, V. L., Wang, S., Fleming, E. L., López-Puertas, M., Funke, B., and

35 Bernath, P. F.: Middle atmospheric changes caused by the January and March 2012 solar proton events, Atmos.

36 Chem. Phys., 14, 1025–1038, https://doi.org/10.5194/acp-14-1025-2014, 2014.

37 Kalakoski, N., Verronen, P. T., Seppälä, A., Szeląg, M. E., Kero, A., and Marsh, D. R.: Statistical response of

38 middle atmosphere composition to solar proton events in WACCM-D simulations: importance of lower iono-

39 spheric chemistry, Atmos. Chem. Phys. Discuss., https://doi.org/10.5194/acp-2019-1133, in review, 2020.

1   Livesey, N. J., Read, W. G., Froidevaux, L., Lambert, A., Manney, G. L., Pumphrey, H. C., Santee, M. L.,
2   Schwartz, M. J., Wang, S., Cofield, R. E., Cuddy, D. T., Fuller, R. A., Jarnot, R. F., Jiang, J. H., Knosp, B. W.,
3   Stek, P. C., Wagner, P. A., and Wu, D. L.: EOS MLS Version 4.2x Level 2 data quality and description doc-
4   ument, Tech. rep., Jet Propulsion Laboratory D-33509 Rev. D, available at: http://mls.jpl.nasa.gov/, 2018.
5   Manney, G. L., Santee, M. L, Rex, M., Livesey, N. J., Pitts, M. C., Veefkind, P., Nash, E. R., Wohltmann, I.,
6   Lehmann, R., Froidevaux, L., Poole, L. R., Schoeberl, M. R., Haffner, D. P., Davies, J., Dorokhov, V., Gernandt,
7   H., Johnson, B., Kivi, R., Kyrö, E., Larsen, N., Levelt, P. F., Makshtas, A., McElroy, C. T., Nakajima, H., Par-
8   rondo, M. C., Tarasick, D. W., von der Gathen, P., Walker, K. A., and Zinoviev, N. S.: Unprecedented Arctic
9   ozone loss in 2011, Nature, 478, 469–475, https://doi.org/10.1038/nature10556, 2011.
10   Marsh, D. R., Garcia, R. R., Kinnison, D. E., Boville, B. A., Sassi, F., Solomon, S. C., and Matthes, K.: Modeling
11   the whole atmosphere response to solar cycle changes in radiative and geomagnetic forcing, J. Geophys. Res.
12   (Atmos.), 112, D23306, https://doi.org/10.1029/2006JD008306, 2007.
13   Marsh, D. R., Mills, M., Kinnison, D., Lamarque, J.-F., Calvo, N., and Polvani, L.: Climate change from 1850 to
14   2005 simulated in CESM1(WACCM), J. Climate, 26, 7372–7391, https://doi.org/10.1175/JCLI-D-12-00558.1,
15   2013.
16   Matthes, K., Funke, B., Andersson, M. E., Barnard, L., Beer, J., Charbonneau, P., Clilverd, M. A., Dudok de Wit,
17   T., Haber- reiter, M., Hendry, A., Jackman, C. H., Kretzschmar, M., Kr- uschke, T., Kunze, M., Langematz, U.,
18   Marsh, D. R., May- cock, A. C., Misios, S., Rodger, C. J., Scaife, A. A., Seppälä, A., Shangguan, M., Sinnhuber,
19   M., Tourpali, K., Usoskin, I., van de Kamp, M., Verronen, P. T., and Versick, S.: Solar forcing for CMIP6 (v3.2),
20   Geosci. Model Dev., 10, 2247–2302, https://doi.org/10.5194/gmd-10-2247-2017, 2017.
21   Päivärinta, S., Verronen, P., Funke, B., Gardini, A., Seppälä, A., and Andersson, M.: Transport versus energetic
22   particle precipitation: Northern polar stratospheric NOx and ozone in January–March 2012, J. Geophys. Res.-
23   Atmos., 121, 6085–6100, https://doi.org/10.1002/2015JD024217, 2016.
24   Pommereau, J. P., Goutail, F., Pazmino, A., Lefevre, F., Chipperfield, M. P., Feng, W. H., Van Roozendael, M.,
25   Jepsen, N., Hansen, G., Kivi, R., Bognar, K., Strong, K., Walker, K., Kuzmichev, A., Khattatov, S., and Sitnikova,
26   V.: Recent Arctic ozone depletion: Is there an impact of climate change? Comptes Rendus Geoscience, 350 (7),
27   347-353, https://doi.org/10.1016/j.crte.2018.07.009, 2018.
28   Randall, C. E., Harvey, V. L., Singleton, C. S., Bailey, S. M., Bernath, P. F., Codrescu, M., Nakajima, H., and
29   Russell, J. M.: Energetic particle precipitation effects on the Southern Hemisphere stratosphere in 1992–2005, J.
30   Geophys. Res., 112, D08308, https://doi.org/10.1029/2006JD007696, 2007.
31   Rienecker, M. M., Suarez, M. J., Gelaro, R., Todling, R., Bacmeister, J., Liu, E., Bosilovich, M. G., Schubert, S.
32   D., Takacs, L., Kim, G.-K., Bloom, S., Chen, J., Collins, D., Conaty, A., da Silva, A., Gu, W., Joiner, J., Koster,
33   R. D., Lucchesi, R., Molod, A., Owens, T., Pawson, S., Pegion, P., Redder, C. R., Reichle, R., Robertson, F. R.,
34   Ruddick, A. G., Sienkiewicz, M., and Woollen, J.: MERRA – NASA's Modern-Era Retrospective Analysis for
35   Research and Applications, J. Climate, 24, 3624–3648, https://doi.org/10.1175/JCLI-D-11-00015.1, 2011.
36   Seppälä, A., Verronen, P. T., Kyrölä, E., Hassinen, S., Back- man, L., Hauchecorne, A., Bertaux, J. L., and Fussen,
37   D.: Solar proton events of October–November 2003: Ozone depletion in the Northern Hemisphere polar winter
38   as seen by GOMOS/Envisat, Geophys. Res. Lett., 31, L19107, https://doi.org/10.1029/2004GL021042, 2004.
39   Sinnhuber, M., Nieder, H., and Wieters, N.: Energetic Particle Precipitation and the Chemistry of the Meso-
40   sphere/Lower Thermosphere. Surv Geophys 33, 1281–1334, https://doi.org/10.1007/s10712-012-9201-3, 2012.

Sinnhuber, M., Berger, U., Funke, B., Nieder, H., Reddmann, T., Stiller, G., Versick, S., von Clarmann, T., and Wissing, J. M.: NOy production, ozone loss and changes in net radiative heat- ing due to energetic particle pre- cipitation in 2002–2010, Atmos. Chem. Phys., 18, 1115–1147, https://doi.org/10.5194/acp-18-1115-2018, 2018.

Stone, K. A., Solomon, S., and Kinnison, D. E.: On the Identifi- cation of Ozone Recovery, Geophys. Res. Lett., 45, 5158–5165, https://doi.org/10.1029/2018GL077955, 2018

Usoskin, I. G., Kovaltsov, G. A., Mironova, I. A., Tylka, A. J., and Dietrich, W. F.: Ionization effect of solar particle GLE events in low and middle atmosphere, Atmos. Chem. Phys., 11, 1979–1988, https://doi.org/10.5194/acp-11-1979-2011, 2011.

Verronen, P. T., Seppälä, A., Kyrola, E., Tamminen, J., Pickett, H. M., and Turunen, E.: Production of odd hy- drogen in the meso- sphere during the January 2005 solar proton event, Geophys. Res. Lett., 33, L24811, https://doi.org/10.1029/2006GL028115, 2006.

Verronen, P. T. and Lehmann, R.: Analysis and parameterisation of ionic reactions affecting middle atmospheric HOx and NOy during solar proton events, Ann. Geophys., 31, 909–956, https://doi.org/10.5194/angeo-31-909- 2013, 2013.

Verronen, P. T., Andersson, M. E., Marsh, D. R., Kovács, T., and Plane, J. M. C.: WACCM-D – Whole Atmos- phere Community Climate Model with D-region ion chemistry, J. Adv. Model. Earth Sy., 8, 954–975, https://doi.org/10.1002/2015MS000592, 2016.

Waters, J. W., Froidevaux, L., Harwood, R. S., Jarnot, R. F., Pickett, H. M., Read, W. G., Siegel, P. H., Cofield, R. E., Filipiak, M. J., Flower, D. A., Holden, J. R., Lau, G. K. K., Livesey, N. J., Manney, G. L., Pumphrey, H. C., Santee, M. L., Wu, D. L., Cuddy, D. T., Lay, R. R., Loo, M. S., Perun, V. S., Schwartz, M. J., Stek, P. C., Thurstans, R. P., Boyles, M. A., Chandra, K. M., Chavez, M. C., Chen, G. S., Chudasama, B. V., Dodge, R., Fuller, R. A., Girard, M. A., Jiang, J. H., Jiang, Y. B., Knosp, B. W., LaBelle, R. C., Lam, J. C., Lee, K. A., Miller, D., Oswald, J. E., Patel, N. C., Pukala, D. M., Quintero, O., Scaff, D. M., Van Snyder, W., Tope, M. C., Wagner, P. A., and Walch, M. J.: The Earth Observing System Microwave Limb Sounder (EOS MLS) on the Aura satellite, IEEE Trans. Geosci. Remote Sens., 44, 1075–1092, https://doi.org/10.1109/TGRS.2006.873771, 2006.